J. Appl. Comput. Mech., 5(4) (2019) 779-790
DOI: 10.22055/JACM.2019.27524.1412

ISSN: 2383-4536
jacm.scu.ac.ir

M&MoCS

Shahid Chamran University of Ahvaz

Journal of Applied and Computational Mechanics

Research Paper

Transient Electro-osmotic Slip Flow of an Oldroyd-B Fluid with Time-fractional Caputo-Fabrizio Derivative

Nehad Ali Shah[1,2], Xiaoping Wang[3], Haitao Qi[3], Shaowei Wang[4], Ahmad Hajizadeh[5,6]

[1] Department of Mathematics, Lahore Leads University, Lahore Pakistan
[2] Abdus Salam School of Mathematical Sciences, GC University, Lahore, 54600, Pakistan
[3] School of Mathematics and Statistics, Shandong University, Weihai, 264209, PR China
[4] School of Civil Engineering, Shandong University, Jinan, 250061, PR China
[5] FAST, University Tun Hussein Onn Malaysia, 86400, Parit Raja, Batu Pahat, Johor State, Malaysia
[6] Public Authority of Applied Education and Training, College of Technological Studies, Applied Science Department, Shuwaikh, Kuwait

Received November 04 2018; Revised February 12 2019; Accepted for publication February 13 2019.
Corresponding author: Nehad Ali Shah, nehadali199@sms.edu.pk

Abstract. In this article, the electro-osmotic flow of Oldroyd-B fluid in a circular micro-channel with slip boundary condition is considered. The corresponding fractional system is represented by using a newly defined time-fractional Caputo-Fabrizio derivative without singular kernel. Closed form solutions for the velocity field are acquired by means of Laplace and finite Hankel transforms. Additionally, Stehfest's algorithm is used for inverse Laplace transform. The solutions for fractional Maxwell, ordinary Maxwell and ordinary Newtonian fluids are obtained as limiting cases of the obtained solution. Finally, the influence of fractional and some important physical parameters on the fluid flow are spotlighted graphically.

Keywords: Electro-osmotic flow; Slip boundary condition; Oldroyd-B fluid; Time-fractional Caputo-Fabrizio derivative; Stehfest's algorithm.

1. Introduction

Electro-osmosis phenomenon refers to bulk movement of an aqueous solution past a stationary solid surface due to an externally applied electric field [1]. It is used intensified in the context of micro and nano fluidics and in enormous scientific applications such as lab-on-a-chip technologies, soil analysis and chemical analysis [2]. Towards its potential applications, many theoretical [3-9], numerical [10, 11] and experimental [12, 13] studies on different electro-osmotic flow models are carried out by many authors for Newtonian and non-Newtonian fluids.

The subject of fractional calculus deals with the integrals and derivatives of any arbitrary real number. It has powerful applications in physics, engineering and many scientific areas [14-16]. The fractional derivative has many definitions, namely, Riemann-Liouville time-fractional derivative, Caputo time-fractional derivative [17], more recently, Caputo and Fabrizio [18]. The first two definitions, Riemann-Liouville time-fractional derivative, Caputo time-fractional derivative have a singular kernel while the new definition of the Caputo and Fabrizio time-fractional derivative is without singular kernal. Losada and Nieto [19] introduced the fractional integer corresponding to the fractional Caputo- Fabrizio derivative and studied its related fractional differential equations. In addition, Alsaedi *et al.* [20] found the solutions for a coupled system of time-fractional differential equations including continuous functions and the Caputo-Fabrizio fractional derivative. Moreover, Baleanu *et al.* [21] applied the variational homotopic perturbation and q-homotopic analysis methods to make a comparison between Caputo and Caputo-Fabrizio derivatives for the time-fractional advection equation. They indicated that rough answers for both derivatives are similar and the Caputo–Fabrizio derivative is faster than the Caputo derivative in terms of CPU speed up

Published online: May 10 2019

computations by using Mathematica.

Recently, the fluid flow with fractional derivatives becomes a highly emerging area of research. The effect of fractional parameter for different fluids has been studied by many researchers [22-25]. They described the governing equations by the corresponding fractional partial differential equations and then they obtained exact solutions by using the discrete Laplace transform, Fourier transform and some well-known special functions. Several researchers discussed Oldroyd-B fluid models by means of fractional approaches. Zheng *et al.* [26] illustrated the slip effects on the magnetohydrodynamic flow of an incompressible generalized Oldroyd-B fluid induced by an accelerating plate by using fractional calculus approach. They introduced closed form solutions for velocity and shear stress in terms of Fox H-function by using the discrete Laplace transform of the sequential fractional derivatives. Exact solutions for the helical flow of a generalized Oldroyd-B fluid in a circular cylinder by using Hankel and Laplace transforms are obtained by Fetecau *et al.* [27]. Qi and Xu [28] used the discrete Laplace transform of the sequential fractional derivative for the flow near a wall suddenly set in motion for a viscoelastic fluid with the generalized Oldroyd-B model. For the electro-osmotic flow of the Oldroyd-B fluid model, Jiang *et al.* [29] studied the electro-osmotic flow of a fractional Oldroyd-B fluid in a circular microchannel with linear Navier slip velocity boundary condition. They derived exact solutions for the electric potential and transient velocity by means of Laplace and finite Hankel transforms. Moreover, they obtained the solutions for the fractional Maxwell fluid and fractional second grade fluid as well as Newtonian fluid as special cases from the main results. Other interesting and recent solutions regard electro-osmotic flow with time-fractional derivative obtained in [30-33] by considering different types of fluids.

This article is concerned with studying the electro-osmotic flow of an Oldroyd-B fluid with slip boundary condition in a circular micro-channel by using a newly defined time-fractional Caputo-Fabrizio derivative without singular kernel. Closed form solutions for velocity are obtained by using Laplace and finite Hankel transforms. In addition, Stehfest's algorithm is used for inverse Laplace transform. The solutions for fractional Maxwell, ordinary Maxwell and ordinary Newtonian fluids are obtained as special cases of the general solution. Finally, the influences of the fractional parameter as well as some other important physical parameters on the fluid flow are spotlighted graphically. Our results may be useful for the prediction of the flow behavior of viscoelastic fluids in micro-channels and can benefit the design of micro-fluidic devices.

2. Formulation of the Problem and Governing Equation

The continuity equation for an incompressible viscoelastic fluid is

$$\nabla . \vec{\mathrm{V}} = 0 \tag{1}$$

We consider the flow of an Oldroyd-B fluid in a straight circular cylinder. The velocity field is defined as

$$\vec{\mathrm{V}} = \mathrm{v}_r \vec{e}_r + \mathrm{v}_\theta \vec{e}_\theta + \mathrm{v}_z \vec{e}_z , \quad \text{with } \ \mathrm{v}_r = 0,\ \mathrm{v}_\theta = 0,\ \mathrm{v}_z = u(r,t) \tag{2}$$

The constitutive equation is

$$\left(1+\lambda \frac{\partial}{\partial t}\right)\tau(r,t) = \mu\left(1+\lambda_r \frac{\partial}{\partial t}\right)\frac{\partial u(r,t)}{\partial r} \tag{3}$$

where, $\tau = T_{rz}$ is the shear stress, λ and λ_r are the relaxation and retardation time, respectively, and μ is the constant viscosity. The start-up from rest of the electro-osmotic flow of a viscoelastic fluid in a circular microchannel of radius *R*. The dielectric constant of the fluid is ε. It is assumed that the channel wall is uniformly charged with a zeta potential ψ_W, and the liquid solution is a viscoelastic fluid whose behavior can be described by the fractional Oldroyd-B (Jeffrey's) equation (3). When the external electric field E_0 is imposed along the axial direction, then the fluid in the micro-channel sets in motion due to the electro-osmosis.

According to the theory of electrostatics, the net change density ρ_e is expressed by a potential distribution ψ, which is given by the following equation of Poisson type

$$\Delta^2 \psi = -\frac{\rho_e}{\varepsilon} \Leftrightarrow \Delta \psi = -\frac{\rho_e}{\varepsilon} \tag{4}$$

The corresponding boundary conditions of the zeta potential are

$$\psi(R,\theta) = \psi_W , \quad \left.\frac{\partial \psi}{\partial r}\right|_{r=0} = 0. \tag{5}$$

Also, assume that the change distribution in the Debye layer is not affected by time, therefore, the wall of the channel has constant electric potential E_0. In the assumption of the Boltzmann distribution and a small surface (zeta) potential of the electrical double-layer, we use the Debye-Huckel approximation, so

$$\rho_e = -\frac{2 z_\upsilon^2 e^2 n_0}{k_B T}\psi \tag{6}$$

where n_0 is the bulk number concentration, z_υ is the valence of ions, e is the fundamental charge, k_B is the Boltzmann constant, T is the absolute temperature.

$$\Delta f = \frac{1}{r}\frac{\partial}{\partial r}\left(r\frac{\partial f}{\partial r}\right)+\frac{1}{r^2}\frac{\partial^2 f}{\partial \theta^2}+\frac{\partial^2 f}{\partial z^2} \tag{7}$$

if $f = f(r,t)$ (in our problem all functions depend only of (r,t)). Implies that

$$\Delta f = \frac{1}{r}\frac{\partial}{\partial r}\left(r\frac{\partial f}{\partial r}\right)=\frac{1}{r}\left(\frac{\partial f}{\partial r}+r\frac{\partial^2 f}{\partial r^2}\right)=\frac{\partial^2 f}{\partial r^2}+\frac{1}{r}\frac{\partial f}{\partial r} \tag{8}$$

By using (6) and (8) in (4) we have

$$\frac{\partial^2\psi}{\partial r^2}+\frac{1}{r}\frac{\partial\psi}{\partial r}=-\frac{1}{\varepsilon}\frac{-2z_\upsilon^2e^2n_0}{k_BT}\psi \tag{9}$$

We define $k^2=(2z_\upsilon^2e^2n_0)/(\varepsilon k_BT)$, the Debye-Huckel parameter and equation for the electrical potential ψ becomes

$$\frac{\partial^2\psi}{\partial r^2}+\frac{1}{r}\frac{\partial\psi}{\partial r}-k^2\psi=0, \quad \text{or} \quad r^2\frac{\partial^2\psi}{\partial r^2}+r\frac{\partial\psi}{\partial r}-(k^2r^2+0^2)\psi=0 \tag{10}$$

Eq. (10) is the modified Bessel equation with the general solution

$$\psi(r)=C_1I_0(kr)+C_2K_0(kr) \tag{11}$$

By using

$$\frac{d}{dr}I_0(u(r))=I_1(u(r))u'(r); \quad \frac{d}{dr}K_0(u(r))=-K_1(u(r))u'(r), \tag{12a}$$

$$\frac{\partial\psi}{\partial r}=C_1kI_1(kr)-C_2kK_1(kr) \tag{12b}$$

Since, $\lim_{r\to 0}K_1(kr)=\infty,\ I_1(0)=0,\ C_2$ must be zero.

$$\psi(r)=C_1I_0(kr) \tag{13a}$$

$$r=R \Rightarrow C_1I_0(kR)=\psi_W \Rightarrow C_1=\frac{\psi_W}{I_0(kR)} \tag{13b}$$

Finally, the solution of (3) and (4) is obtained as

$$\psi(r)=\psi_W\frac{I_0(kr)}{I_0(kR)} \tag{14}$$

The relevant equation of the linear momentum is

$$\rho\frac{\partial u}{\partial t}=\frac{1}{r}\frac{\partial}{\partial r}(r\tau_{rz})+\rho_eE_0, \quad \text{or} \quad \rho\frac{\partial u}{\partial t}=\frac{1}{r}\tau_{rz}+\frac{\partial\tau_{rz}}{\partial r}+\rho_eE_0 \tag{15}$$

But, $\rho_e=-(2z_\upsilon^2e^2n_0)\psi/(k_BT)=-\varepsilon k^2\psi=-\varepsilon k^2\psi_WI_0(kr)/I_0(kR)$, then, Eq. (15) becomes

$$\rho\frac{\partial u}{\partial t}=\frac{1}{r}\tau+\frac{\partial\tau}{\partial r}-\varepsilon k^2\psi_WE_0I_0(kr)/I_0(kR) \tag{16}$$

The constitutive and linear momentum equations for ordinary Oldroyd-B fluid are:
The constitutive equation:

$$\left(1+\lambda\frac{\partial}{\partial t}\right)\tau=\mu\left(1+\lambda_r\frac{\partial}{\partial t}\right)\frac{\partial u}{\partial r}, \tag{17}$$

The linear momentum equation:

$$\rho\frac{\partial u}{\partial t}=\frac{1}{r}\frac{\partial(\tau r)}{\partial r}-\varepsilon k^2\psi_WE_0I_0(kr)/I_0(kR) \tag{18}$$

the initial conditions are written as

$$u(r,0)=0,\ \left.\frac{\partial u(r,t)}{\partial t}\right|_{t=0}=0, \tag{19}$$

the boundary conditions are

$$\left.\frac{\partial u(r,t)}{\partial r}\right|_{r=0}=0,\ u(R,t)+d\left.\frac{\partial u(r,t)}{\partial r}\right|_{r=R}=0. \tag{20}$$

By introducing the following non-dimensional variables

$$\psi^*=\frac{\psi}{\psi_W},u^*=\frac{u}{u_s},r^*=\frac{r}{R},t^*=\frac{\nu}{R^2}t,d^*=\frac{d}{R},\lambda^*=\frac{\nu\lambda}{R^2},\lambda_r^*=\frac{\nu\lambda_r}{R^2},u_s=-\frac{\varepsilon\psi_W E_0}{\mu},\tau^*=\frac{R\tau}{\mu u_s}, \tag{21}$$

after dropping the star notation, we can obtain the basic equation for Oldroyd-B fluid in the following non-dimensional form

$$\left.\begin{aligned}&\left(1+\lambda\frac{\partial}{\partial t}\right)\tau=\left(1+\lambda_r\frac{\partial}{\partial t}\right)\frac{\partial u}{\partial r},\quad \frac{\partial u}{\partial t}=\frac{1}{r}\frac{\partial(r\tau)}{\partial r}+K^2\frac{I_0(Kr)}{I_0(K)},\left.\frac{\partial u(r,t)}{\partial r}\right|_{r=0}=0,\\&u(1,t)+d\left.\frac{\partial u(r,t)}{\partial r}\right|_{r=1}=0.\end{aligned}\right\} \tag{22}$$

2.1. The fractional model with Caputo-Fabrizio derivatives

In this case, the constitutive equation is

$$\left(1+\lambda D_t^{\alpha}\right)\tau(r,t)=\left(1+\lambda_r D_t^{\beta}\right)\frac{\partial u(r,t)}{\partial r},\quad 0\le\alpha\le 1,\quad 0\le\beta\le 1. \tag{23}$$

By applying the operator $(1+\lambda D_t^{\alpha})$ to Eq. (22), the obtained result can be written as

$$\left(1+\lambda D_t^{\alpha}\right)\frac{\partial u}{\partial t}=\frac{1}{r}\frac{\partial}{\partial r}\left[r\left(1+\lambda D_t^{\alpha}\right)\tau\right]+\left(1+\lambda D_t^{\alpha}\right)\frac{K^2 I_0(Kr)}{I_0(K)} \tag{24}$$

By using equation (16) and the property $D_t^{\alpha}C=0, C=$ Constant, the result reduce to the following form,

$$\left(1+\lambda D_t^{\alpha}\right)\frac{\partial u}{\partial t}=\left(1+\lambda_r D_t^{\beta}\right)\frac{1}{r}\frac{\partial}{\partial r}\left[r\frac{\partial u}{\partial r}\right]+\frac{K^2 I_0(Kr)}{I_0(K)} \tag{25}$$

$$u(r,0)=0,\ \left.\frac{\partial u(r,t)}{\partial t}\right|_{t=0}=0, \tag{26}$$

$$\left.\frac{\partial u(r,t)}{\partial r}\right|_{r=0}=0,\ u(1,t)+d\left.\frac{\partial u(r,t)}{\partial r}\right|_{r=1}=0. \tag{27}$$

$$D_t^{\alpha}f(r,t)=\frac{\int_0^t e^{-\frac{\alpha(t-\tau)}{1-\alpha}}\frac{\partial f(r,t)}{\partial\tau}d\tau}{1-\alpha}=\left(\frac{e^{\frac{-\alpha t}{1-\alpha}}}{1-\alpha}\right)*\left(\frac{\partial f(r,t)}{\partial t}\right) \tag{28}$$

$$L\left\{D_t^{\alpha}f(r,t)\right\}=L\left\{\frac{e^{\frac{-\alpha t}{1-\alpha}}}{1-\alpha}\right\}L\left\{\frac{\partial f(r,t)}{\partial t}\right\}=\frac{1}{1-\alpha}\frac{1}{s+\frac{\alpha}{1-\alpha}}\left[sL\left\{f(r,t)\right\}-f(r,0)\right]=\frac{sL\left\{f(r,t)\right\}-f(r,0)}{(1-\alpha)s+\alpha} \tag{29}$$

Then, Eq. (25) becomes

$$\frac{\partial u}{\partial t}+\lambda D_t^{\alpha}\frac{\partial u}{\partial t}=\frac{1}{r}\frac{\partial}{\partial r}\left[r\frac{\partial u}{\partial r}\right]+\lambda_r\frac{1}{r}\frac{\partial}{\partial r}\left[rD_t^{\beta}\frac{\partial u}{\partial r}\right]+\frac{K^2 I_0(Kr)}{I_0(K)} \tag{30a}$$

$$L\left\{D_t^{\alpha}u(r,t)\right\}=\frac{sL\left\{u(r,t)\right\}-u(r,0)}{(1-\alpha)s+\alpha}=\frac{s\bar{u}(r,t)}{(1-\alpha)s+\alpha}, \tag{30b}$$

$$L\left\{D_t^{\alpha}\frac{\partial u(r,t)}{\partial t}\right\}=\frac{sL\left\{\frac{\partial u(r,t)}{\partial t}\right\}-\left.\frac{\partial u(r,t)}{\partial t}\right|_{t=0}}{(1-\alpha)s+\alpha}=\frac{s\left[s\bar{u}(r,s)-u(r,0)\right]}{(1-\alpha)s+\alpha}=\frac{s^2\bar{u}(r,t)}{(1-\alpha)s+\alpha}, \tag{30c}$$

where $\bar{u}(r,s)=\int_0^{\infty}u(r,t)e^{-st}dt$ is the Laplace transform of the function $u(r,t)$.

3. Solution of the Problem

By applying the Laplace transform to Eq. (18), the solution in transform domain is

$$\frac{(1-\alpha+\lambda)s^2+\alpha s}{(1-\alpha)s+\alpha}\bar{u}(r,s)=\frac{(1-\beta+\lambda_r)s+\beta}{(1-\beta)s+\beta}\frac{1}{r}\frac{\partial}{\partial r}\left(r\frac{\partial\bar{u}(r,s)}{\partial r}\right)+\frac{K^2}{s}\frac{I_0(Kr)}{I_0(K)}, \tag{31}$$

or

$$\bar{u}(r,s)=\frac{\left[(1-\beta+\lambda_r)s+\beta\right]\left[(1-\alpha)s+\alpha\right]}{\left[(1-\beta)s+\beta\right]\left[(1-\alpha+\lambda)s^2+\alpha s\right]}\frac{1}{r}\frac{\partial}{\partial r}\left(r\frac{\partial\bar{u}(r,s)}{\partial r}\right)+\frac{\left[(1-\alpha)s+\alpha\right]K^2}{s\left[(1-\alpha+\lambda)s^2+\alpha s\right]}\frac{I_0(Kr)}{I_0(K)}, \tag{32}$$

By applying Hankel transform and rearrange the following results is obtain

$$\bar{u}_H(r_n,s)=\bar{U}_n(s)\frac{J_0(r_n)}{r_n^2+K^2} \tag{33}$$

where

$$\bar{U}_n(s)=\frac{\left[(1-\alpha)s+\alpha\right]\left[a_0s^2+b_0s+c_0\right]}{s\left[(1-\alpha+\lambda)s+\alpha\right]\left[a_0s^3+a_{1n}s^2+a_{2n}s+a_{3n}\right]}\gamma_0,$$

$$a_0=(1-\beta)(1-\alpha+\lambda),$$

$$b_0=\alpha(1-\beta)+\beta(1-\alpha+\lambda),\;\; c_0=\alpha\beta, \tag{34}$$

$$a_{1n}=\alpha(1-\beta)+\beta(1-\alpha+\lambda)+(1-\alpha)(1-\beta+\lambda_r)r_n^2,$$

$$a_{2n}=\alpha\beta+\left[\beta(1-\alpha)+\alpha(1-\beta+\lambda_r)\right]r_n^2,\;\; a_{2n}=\alpha\beta r_n^2,\;\; \gamma_0=\frac{K^2\left(dKI_1(K)+I_0(K)\right)}{dI_0(K)}.$$

Rearrange Eq. (23), such that $u(r,t)$ satisfies the initial and the boundary conditions. First consider the auxiliary function

$$h(r)=\frac{I_0(Kr)}{I_0(K)}-dK\frac{I_1(K)}{I_0(K)}-1 \tag{35}$$

the Hankel transform

$$h_n=\frac{J_1(r_n)}{I_0(K)}\frac{\left(r_n-r_n^2-K^2\right)I_0(K)-dK^2I_1(K)}{r_n(r_n^2+K^2)}, \tag{36}$$

and we have

$$\bar{u}_H(r_n,s)=\frac{\Gamma(3)}{s^3}h_n+\left(\bar{U}_n(s)\frac{J_0(r_n)}{r_n^2+K^2}-\frac{\Gamma(3)}{s^3}h_n\right) \tag{37a}$$

or

$$\bar{u}_H(r_n,s)=\frac{\Gamma(3)}{s^3}h_n+A_n(s) \tag{37b}$$

where $A_n(s)=\bar{U}_n(s)J_0(r_n)/(r_n^2+K^2)-h_n\Gamma(3)/s^3$ with inverse Laplace transform

$$a_n(t)=L^{-1}\{A_n(s)\}=\frac{\ln(2)}{t}\sum_{j=1}^{2p}d_jA_n\left(j\frac{\ln(2)}{t}\right), \tag{38a}$$

$$d_j = (-1)^{j+p} \sum_{i=\left[\frac{j+1}{2}\right]}^{\min(j.p)} \frac{i^p (2n)!}{(p-i)!i!(i-1)!(j-i)!(2i-j)!} \tag{38b}$$

where, [(*j*+1)/2] is the integer part of (*j*+1)/2 and *p* is a positive integer number. By applying the inverse Laplace transform to Eq. (25), results that

$$\bar{u}_H(r_n,t) = t^2 h_n + a_n(t) \tag{39}$$

By applying the inverse Hankel transform to Eq. (27), results that

$$u(r_n,t) = t^2 h(r) + 2\sum_{n=1}^{\infty} \frac{r_n^2 J_0(rr_n)}{\left(r_n^2 + \frac{1}{d^2}\right) J_0^2(r_n)} a_n(t) \tag{40}$$

3.1. Some observations

1. It is observed that $a_n(0) = 0$ and $\left.\frac{da_n(t)}{dt}\right|_{t=0} = 0,$ implies that $u(r,0) = 0$ and $\left.\frac{du(r,t)}{dt}\right|_{t=0} = 0.$
2. Using $h(r)$ and $\left.\frac{dJ_0(rr_n)}{dr}\right|_{r=0} = -r_n J_1(rr_n)\Big|_{r=0} = 0,$ implies that $\left.\frac{\partial(r,t)}{\partial r}\right|_{r=0} = 0.$
3. Using $\left[h(r) + d\frac{dh(r)}{dr}\right]_{r=1} = 0$ and $J_0(rr_n) + d\frac{dJ_0(rr_n)}{dr} = J_0(r_n) - dr_n J_1(r_n) = 0,$ implies that $\left[u(r,t) + d\frac{\partial h(r,t)}{\partial r}\right]_{r=1} = 0$.

So these observations imply that the obtained solution in Eq. (28) satisfies the initial and the boundary conditions.

3.2. Particular cases

3.2.1. Ordinary Oldroyd-B fluid

When taking limit $\alpha, \beta \to 1$ of Eqs. (38) and (40), the obtained result can be write as:

$$u(r,t) = t^2 h(r) + 2\sum_{n=1}^{\infty} \frac{r_n^2 J_0(rr_n)}{\left(r_n^2 + \frac{1}{d^2}\right) J_0^2(r_n)} a_n(t) \tag{41}$$

with inverse Laplace transform we have

$$a_n(t) = L^{-1}\{A_n(s)\} = \frac{\ln(2)}{t} \sum_{j=1}^{2p} d_j A_n\left(j\frac{\ln(2)}{t}\right),$$
$$d_j = (-1)^{j+p} \sum_{i=\left[\frac{j+1}{2}\right]}^{\min(j.p)} \frac{i^p (2n)!}{(p-i)!i!(i-1)!(j-i)!(2i-j)!} \tag{42}$$

where, [(*j*+1)/2] is the integer part of (*j*+1)/2 and *p* is a positive integer number which gives the dimensionless velocity expression for the electro-osmotic flow of the ordinary Oldroyd-B fluid.

3.2.2. Fractional Maxwell fluid

By taking the limit $\lambda_r \to 0$ of Eqs. (38) and (40), the obtained result can be write as:

$$u(r,t) = t^2 h(r) + 2\sum_{n=1}^{\infty} \frac{r_n^2 J_0(rr_n)}{\left(r_n^2 + \frac{1}{d^2}\right) J_0^2(r_n)} a_n(t) \tag{43}$$

where

$$\bar{U}_n(s) = \frac{[(1-\alpha)s + \alpha]\left[a_0 s^2 + b_0 s + c_0\right]}{s\,[(1-\alpha+\lambda)s + \alpha]\left[a_0 s^3 + a_{1n} s^2 + a_{2n} s + a_{3n}\right]} \gamma_0,$$
$$a_0 = (1-\beta)(1-\alpha+\lambda), \tag{44}$$

$$b_0 = \alpha(1-\beta)+\beta(1-\alpha+\lambda),\ c_0 = \alpha\beta,$$

$$a_{1n} = \alpha(1-\beta)+\beta(1-\alpha+\lambda)+(1-\alpha)(1-\beta+\lambda_r)r_n^2,$$

$$a_{2n} = \alpha\beta+\left[\beta(1-\alpha)+\alpha(1-\beta+\lambda_r)\right]r_n^2,\ a_{2n} = \alpha\beta r_n^2,\ \gamma_0 = \frac{K^2\left(dKI_1(K)+I_0(K)\right)}{dI_0(K)}.$$

$$A_n(s) = \bar{U}_n(s)J_0(r_n)/(r_n^2+K^2)-h_n\Gamma(3)/s^3$$

with inverse Laplace transform we have

$$a_n(t) = L^{-1}\{A_n(s)\} = \frac{\ln(2)}{t}\sum_{j=1}^{2p} d_j A_n\left(j\frac{\ln(2)}{t}\right),$$

$$d_j = (-1)^{j+p}\sum_{i=\left[\frac{j+1}{2}\right]}^{\min(j.p)}\frac{i^p(2n)!}{(p-i)!i!(i-1)!(j-i)!(2i-j)!} \tag{45}$$

where, $[(j+1)/2]$ is the integer part of $(j+1)/2$ and p is a positive integer number which gives the dimensionless velocity expression for the electro-osmotic flow of Maxwell fluid with fractional derivative.

3.2.3. Ordinary Maxwell fluid

By taking the limit $\lambda_r \to 0$ and $\alpha,\beta \to 1$ of Eqs. (38) and (40), the obtained result can be write as:

$$u(r,t) = t^2h(r)+2\sum_{n=1}^{\infty}\frac{r_n^2J_0(rr_n)}{\left(r_n^2+\frac{1}{d^2}\right)J_0^2(r_n)}a_n(t) \tag{46}$$

where $A_n(s) = \frac{J_0(r_n)}{r_n^2+K^2}\frac{s^2-b_ns-b_nr_n^2}{s^3\left[\lambda s^2+s+r_n^2\right]}$, $b_n = \frac{2\left(r_n-r_n^2-K^2\right)I_0(K)-dK^3I_1(K)}{dr_n^2I_0(K)}$, with inverse Laplace transform one can obtain

$$a_n(t) = L^{-1}\{A_n(s)\} = \frac{\ln(2)}{t}\sum_{j=1}^{2p} d_j A_n\left(j\frac{\ln(2)}{t}\right),$$

$$d_j = (-1)^{j+p}\sum_{i=\left[\frac{j+1}{2}\right]}^{\min(j.p)}\frac{i^p(2n)!}{(p-i)!i!(i-1)!(j-i)!(2i-j)!} \tag{47}$$

where, $[(j+1)/2]$ is the integer part of $(j+1)/2$ and p is a positive integer number which gives the dimensionless velocity expression for the electro-osmotic flow of the ordinary Maxwell fluid.

3.2.4. Ordinary Newtonian fluid

By taking the limit $\lambda,\lambda_r \to 0$ and $\alpha,\beta \to 1$ of Eqs. (38) and (40), the obtained result can be write as

$$u(r,t) = t^2h(r)+2\sum_{n=1}^{\infty}\frac{r_n^2J_0(rr_n)}{\left(r_n^2+\frac{1}{d^2}\right)J_0^2(r_n)}a_n(t) \tag{48}$$

where $A_n(s) = \frac{J_0(r_n)}{r_n^2+K^2}\frac{s^2-b_ns-b_nr_n^2}{s^3\left[\lambda s^2+s+r_n^2\right]}$, $b_n = \frac{2\left(r_n-r_n^2-K^2\right)I_0(K)-dK^3I_1(K)}{dr_n^2I_0(K)}$, with inverse Laplace transform one can obtain

$$a_n(t) = L^{-1}\{A_n(s)\} = \frac{\ln(2)}{t}\sum_{j=1}^{2p} d_j A_n\left(j\frac{\ln(2)}{t}\right),$$

$$d_j = (-1)^{j+p}\sum_{i=\left[\frac{j+1}{2}\right]}^{\min(j.p)}\frac{i^p(2n)!}{(p-i)!i!(i-1)!(j-i)!(2i-j)!} \tag{49}$$

where, $[(j+1)/2]$ is the integer part of $(j+1)/2$ and p is a positive integer number which gives the dimensionless velocity expression for the electro-osmotic flow of the ordinary Newtonian fluid.

4. Numerical Results and Discussion

In this section we present the graphical analysis of the electro-osmotic flow of an Oldroyd-B fluid with a slip boundary condition in a circular micro-channel by using a newly defined time-fractional Caputo-Fabrizio derivative without singular kernel. Numerical results are given to demonstrate the effects of pertinent parameters such as $\alpha, \beta, d, K, \lambda$ and λ_r on the fluid flow velocity.

All parameters, variables and functions are considered non-dimensional. In Fig. 1, we present the effect of the fractional parameter α versus r on the velocity field for two different values of time t. It is observed that for small value of time in Fig. 1a, near the boundary of the cylinder the velocity increases as the fractional parameter α increases while after some critical values of r the velocity decreases as the fractional parameter α increases. But for large value of time in Fig. 1b, the velocity increases as fractional parameter α increases. The effect of the fractional parameter β versus r is presented in Fig. 2. This shows the opposite influence than Fig. 1.

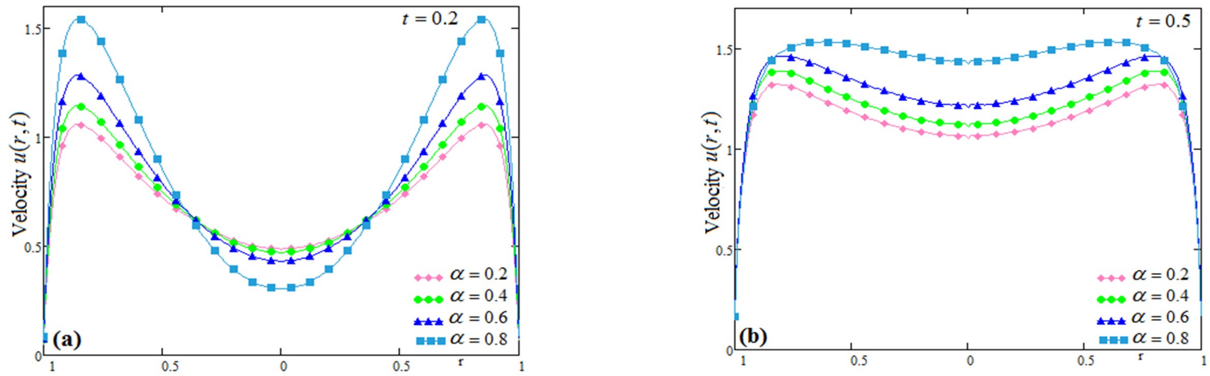

Fig. 1. Profiles of dimensionless velocity against r for α variation at $d = 0.002$, $\lambda = 0.5$, $\lambda_r = 0.1$, K=20, $\beta = 0.8$ and two values of time t.

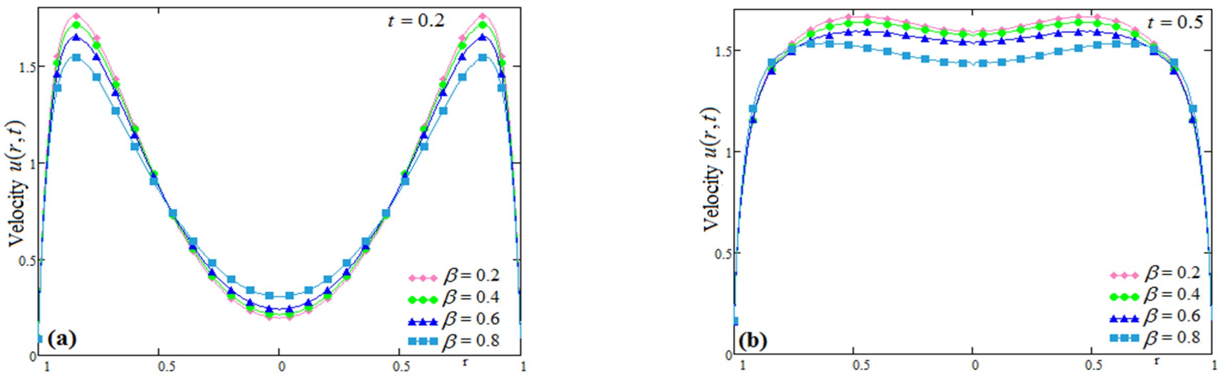

Fig. 2. Profiles of dimensionless velocity against r for β variation at $d = 0.002$, $\lambda = 0.5$, $\lambda_r = 0.1$, K=20, $\alpha = 0.8$ and two values of time t.

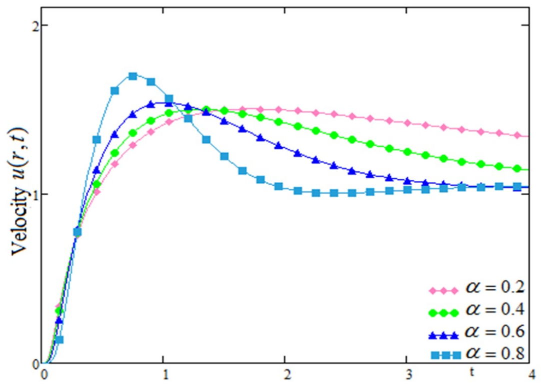

Fig. 3. Profiles of dimensionless velocity against t for α variation at $d = 0.002$, $\lambda = 0.5$, $\lambda_r = 0.1$, K=20, $\beta = 0.8$ and r=0.1

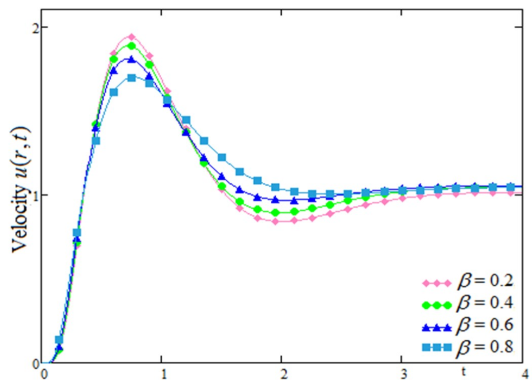

Fig. 4. Profiles of dimensionless velocity against r for β variation at $d = 0.002$, $\lambda = 0.5$, $\lambda_r = 0.1$, K=20, $\alpha = 0.8$ and r=0.1

The effects of fractional parameters α and β versus t on velocity profile are presented in Fig. 3. From this figure one can observe that, for these parameters the fluid behavior is changed at many time values.

In Figs. 5, 6 7, we study the effects of slip, electro-kinetic width and relaxation time, respectively, versus r on fluid flow velocity at two different values of time t. From these figures, it is observed that by increasing the values of slip parameter, the electrokinetic width parameter as well as the relaxation time the velocity increases. It is also important to note that by increasing the time t at the boundary layer difference is increasing.

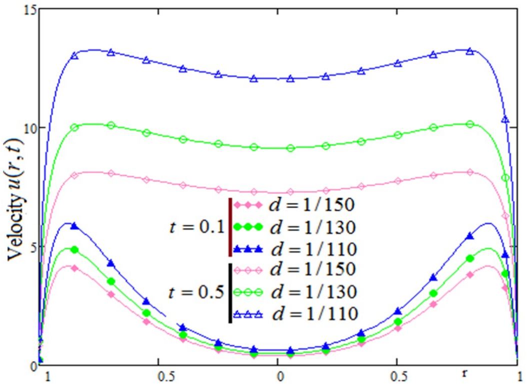

Fig. 5. Profiles of dimensionless velocity against r for d variation at $\lambda = 0.5$, $\lambda_r = 0.1$, K=20, $\alpha = \beta = 0.6$ and two values of time t

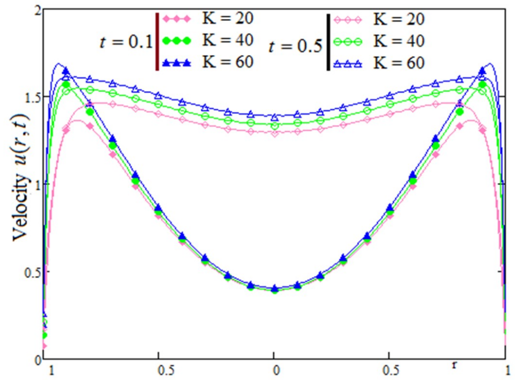

Fig. 6. Profiles of dimensionless velocity against r for K variation at $\lambda = 0.5$, $\lambda_r = 0.1$, d=0.002, $\alpha = \beta = 0.6$ and two values of time t

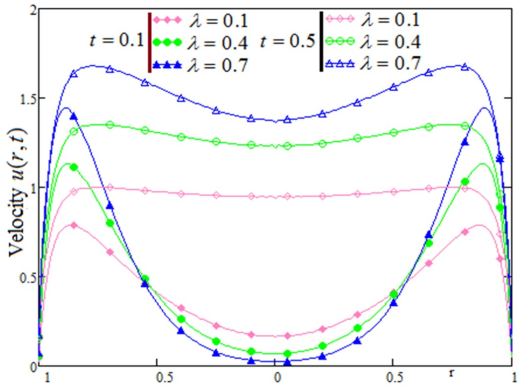

Fig. 7. Profiles of dimensionless velocity against r for λ variation at $d = 0.002$, $\lambda_r = 0.1$, K=20, $\alpha = \beta = 0.6$ and two values of time t

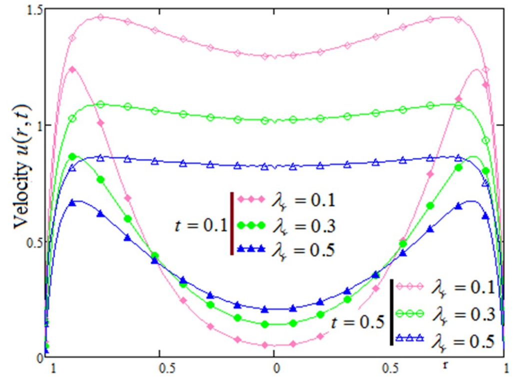

Fig. 8. Profiles of dimensionless velocity against r for λ_r variation at $d = 0.002$, $\lambda = 0.5$, K=20, $\alpha = \beta = 0.6$ and two values of time t

The effect of retardation time λ_r on the velocity profile versus r is presented in Fig. 8. It is observed that by increasing the value of retardation time λ_r the velocity decreases and much influence is appeared for large values of time t. Fig. 8, shows an opposite influence than Figs. 5, 6 and 7.

Figs. 9 and 10 are plotted in order to study the influence of relaxation and retardation time, respectively, versus t at two values of r. From these figures, we observe that initially the velocity has minimum value near the boundary while after some values of time (critical values) the velocity has a maximum value near the boundary.

Similar results are obtained from Figs. 11 and 12 which presented the velocity field when both parameters (r,t) are simultaneous variable and for two values of fractional parameters. The grid points for the plotting are ($r_i = 0.01i$, $t_j = 0.01j$, i, j = 1, 2, …, 100. A comparison between our result and the result of Jiang *et al.* [29] is presented in Fig. 13.

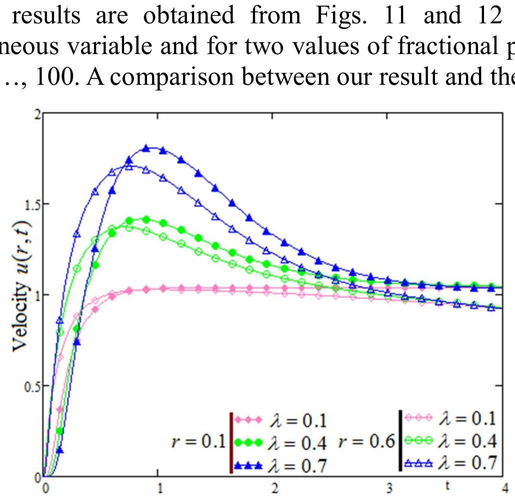

Fig. 9. Profiles of dimensionless velocity against t for λ variation at $d = 0.002$, $\lambda_r = 0.1$, K=20, $\alpha = \beta = 0.6$ and two values of time r

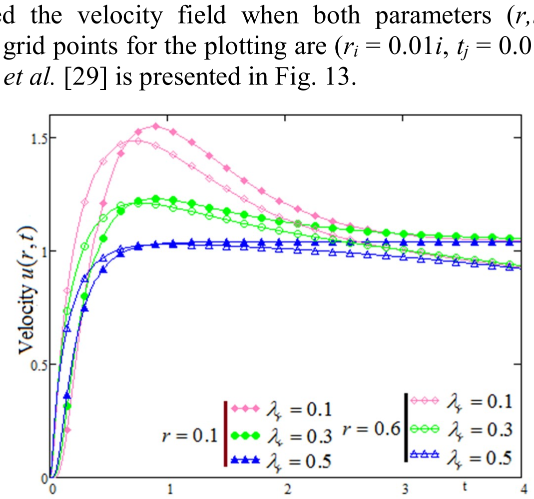

Fig. 10. Profiles of dimensionless velocity against t for λ_r variation at $d = 0.002$, $\lambda = 0.5$, K=20, $\alpha = \beta = 0.6$ and two values of time r

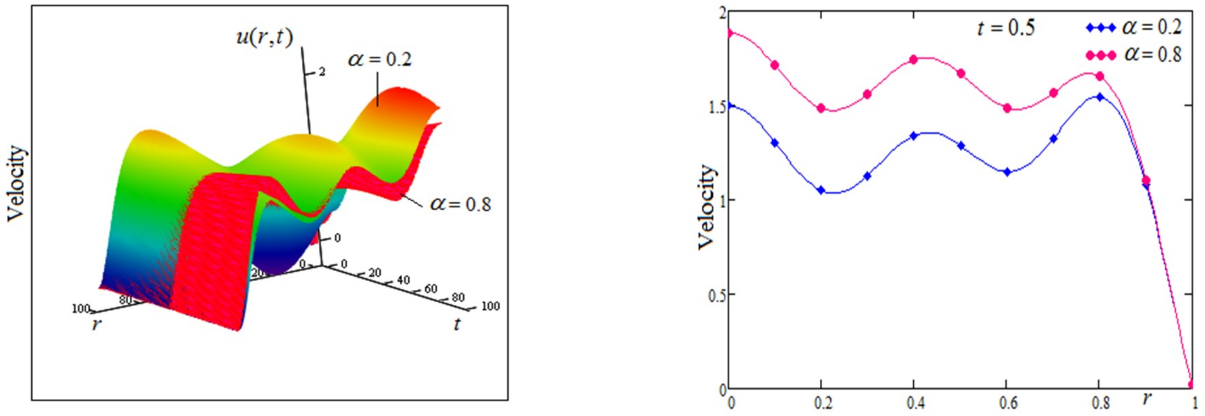

Fig. 11. Variation with r , t and α of the non-dimensional velocity.

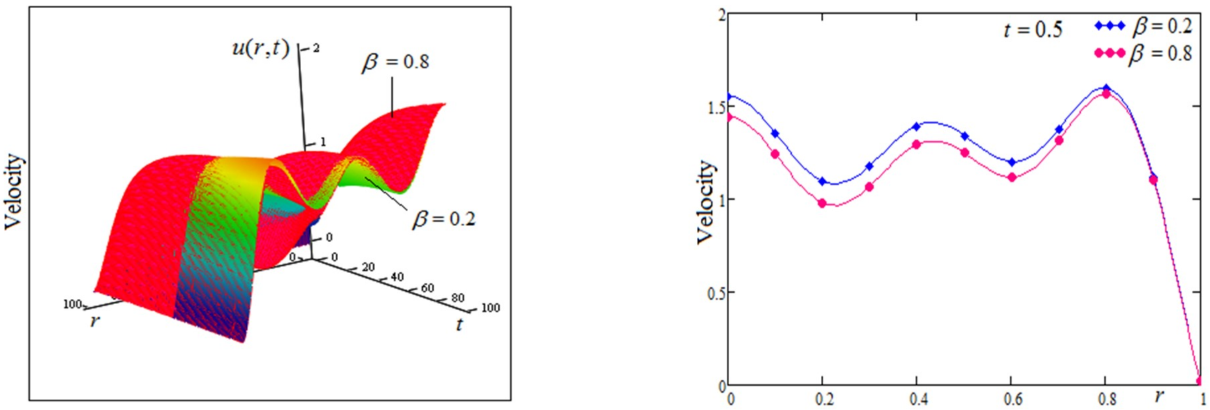

Fig. 12. Variation with r , t and β of the non-dimensional velocity.

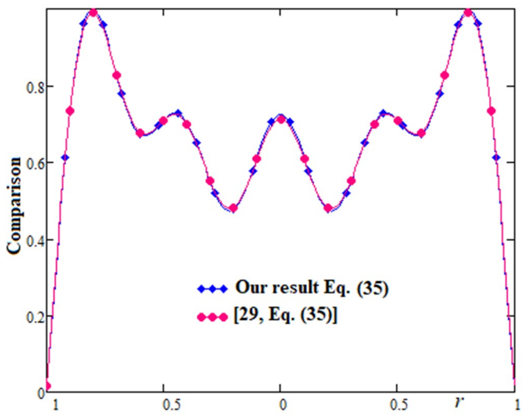

Fig. 13. Comparison of our results with the available similar studies [29].

5. Conclusions

The aim of this article is to study the electro-osmotic flow of an Oldroyd-B fluid with slip condition on the boundary in a circular micro-channel by using time-fractional Caputo-Fabrizio derivative without singular kernel. The Laplace and finite Hankel transforms are used to find solutions for the velocity field. In addition, Stehfest's algorithm is used for inverse Laplace transform. The solutions for fractional Maxwell, ordinary Maxwell and ordinary Newtonian fluids are obtained as limiting cases from the obtained solution. Finally, the influences of the fractional parameter and some important physical parameters on the fluid flow are spotlighted graphically. The following points are observed:

- For small values of time, near the boundary of the cylinder the velocity increased by increasing the values of the fractional parameter α and after some critical values of r the velocity decreased by increasing the values of the fractional parameter α .
- For large values of time, the velocity increased by increasing the values of fractional parameter α .

- For small values of time, near the boundary of the cylinder the velocity decreased by increasing the values of the fractional parameter β and after some critical values of r the velocity increased by increasing the values of the fractional parameter β .
- For large values of time, the velocity decreased by increasing the values of the fractional parameter β .
- By slip, electrokinetic width and relaxation time the velocity increases.
- By increasing the values of retardation time λ_r the velocity decreased and much influence is appeared for large values of time t.

Conflict of Interest

The author(s) declared no potential conflicts of interest with respect to the research, authorship and publication of this article.

Funding

The author Haitao Qi is grateful to National Natural Science Foundation of China (Grant No. 11672163), Natural Science Foundation of Shandong Province, China (Grant Nos. ZR2015AM011) for supporting this work. The author Shaowei Wang is grateful to National Natural Science Foundation of China (Grant No. 11672164) for supporting this work.

Nomenclature

u	Velocity of the fluid,	R	Radius of the channel,
E_0	Electric field strength,	n_0	Bulk ionic number concentration,
d	Slip length,	z_υ	Valence of ions,
e	Electron charge,	T	Absolute temperature,
K	Dimensionless electrokinetic width,	J_0	Bessel function of the first kind,
I_0	Modified Bessel function of the first kind,	r_n	Positive roots of Bessel function of the first kind,
τ	Shear stress,	γ	Shear strain,
μ	Dynamic viscosity,	ρ	Density of the electrolyte solution,
ρ_e	Electric charge density,	λ	Relaxation time,
λ_r	Retardation time,	α,β	Fractional order derivative parameters,
ε	Dielectric constant,	ψ	Potential distribution,
ψ_W	Zeta potential of the channel wall,	k_B	Boltzmann constant,
k	Debye-Huckel parameter,		

References

[1] Ghosal, S., Fluid mechanics of electroosmotic flow and its effect on band broadening in capillary electrophoresis, *Electrophoresis*, 25 (2004) 214-228.
[2] Wang, X., Cheng, C., Wang, S., Liu, S., Electroosmotic pumps and their applications in microfluidic systems, *Microfluidics and Nanofluidics*, 6 (2009) 145.
[3] Bhattacharyya, S., Zheng, Z., Conlisk, A.T., Electro-osmotic flow in two-dimensional charged micro- and nanochannels, *Journal of Fluid Mechanics*, 540 (2005) 247-267.
[4] Wang, C.Y., Liu, Y.H., Chang, C.C., Analytical solution of electroosmotic flow in a semicircular microchannel, *Physics of Fluids*, 20 (2008) 063105.
[5] Chang, S.-H., Electroosmotic flow in a dissimilarly charged slit microchannel containing salt-free solution, *European Journal of Mechanics - B/Fluids*, 34 (2012) 85-90.
[6] Das, S., Chakraborty, S., Analytical solutions for velocity, temperature and concentration distribution in electroosmotic microchannel flows of a non-Newtonian bio-fluid, *Analytica Chimica Acta*, 559 (2006) 15-24.
[7] Chakraborty, S., Electroosmotically driven capillary transport of typical non-Newtonian biofluids in rectangular microchannels, *Analytica Chimica Acta*, 605 (2007) 175-184.
[8] Tan, Z., Qi, H., Jiang, X., Electroosmotic flow of Eyring fluid in slit microchannel with slip boundary condition, *Applied Mathematics and Mechanics*, 35 (2014) 689-696.
[9] Ferrás, L.L., Afonso, A.M., Alves, M.A., Nóbrega, J.M., Pinho, F.T., Analytical and numerical study of the electro-osmotic annular flow of viscoelastic fluids, *Journal of Colloid and Interface Science*, 420 (2014) 152-157.
[10] Tang, G.H., Li, X.F., He, Y.L., Tao, W.Q., Electroosmotic flow of non-Newtonian fluid in microchannels, *Journal of Non-Newtonian Fluid Mechanics*, 157 (2009) 133-137.
[11] Hu, Y., Werner, C., Li, D., Electrokinetic Transport through Rough Microchannels, *Analytical Chemistry*, 75 (2003) 5747-5758.
[12] Sadr, R., Yoda, M., Zheng, Z., Conlisk, A.T., An experimental study of electro-osmotic flow in rectangular microchannels,

Journal of Fluid Mechanics, 506 (2004) 357-367.
[13] Hsieh, S.S., Lin, H.C., Lin, C.Y., Electroosmotic flow velocity measurements in a square microchannel, *Colloid and Polymer Science*, 284 (2006) 1275-1286.
[14] Kulish, V.V., Lage, J.L., Application of Fractional Calculus to Fluid Mechanics, *Journal of Fluids Engineering*, 124 (2002) 803-806.
[15] Tenreiro Machado, J.A., Silva, M.F., Barbosa, R.S., Jesus, I.S.R., Marcos, M.G., Galhano, A.F., Some Applications of Fractional Calculus in Engineering, *Mathematical Problems in Engineering*, 2010 (2010) 1-34.
[16] Debnath, L., Recent applications of fractional calculus to science and engineering, *International Journal of Mathematics and Mathematical Sciences*, 2003 (2003) 3413-3442.
[17] Caputo, M., Linear models of dissipation whose Q is almost frequency independent, Part II, *Geophysical Journal of the Royal Astronomical Society*, 13 (1967) 529-539.
[18] Caputo, M., Fabrizio, M., A new definition of fractional derivative without singular kernel, *Progress in Fractional Differentiation and Applications*, 1 (2015) 73-85.
[19] Losada, J., Nieto, J.J., Properties of a new fractional derivative without singular kernel, *Progress in Fractional Differentiation and Applications*, 1 (2015) 87-92.
[20] Alsaedi, A., Baleanu, D., Etemad, S., Rezapour, S., On Coupled Systems of Time-Fractional Differential Problems by Using a New Fractional Derivative, *Journal of Function Spaces*, 2016 (2016) 8.
[21] Baleanu, D., Agheli, B., Qurashi, M.M.A., Fractional advection differential equation within Caputo and Caputo–Fabrizio derivatives, *Advances in Mechanical Engineering*, 8(12) (2016) 1687814016683305.
[22] Chatterjee, A., Statistical origins of fractional derivatives in viscoelasticity, *Journal of Sound and Vibration*, 284 (2005) 1239-1245.
[23] Kawada, Y., Nagahama, H., Hara, H., Irreversible thermodynamic and viscoelastic model for power-law relaxation and attenuation of rocks, *Tectonophysics*, 427 (2006) 255-263.
[24] Shah, N.A., Khan, I., Heat transfer analysis in a second grade fluid over and oscillating vertical plate using fractional Caputo–Fabrizio derivatives, *The European Physical Journal C*, 76 (2016) 362.
[25] Khan, I., Shah, N.A., Mahsud, Y., Vieru, D., Heat transfer analysis in a Maxwell fluid over an oscillating vertical plate using fractional Caputo-Fabrizio derivatives, *The European Physical Journal Plus*, 132 (2017) 194.
[26] Zheng, L., Liu, Y., Zhang, X., Slip effects on MHD flow of a generalized Oldroyd-B fluid with fractional derivative, *Nonlinear Analysis: Real World Applications*, 13 (2012) 513-523.
[27] Fetecau, C., Mahmood, A., Fetecau, C., Vieru, D., Some exact solutions for the helical flow of a generalized Oldroyd-B fluid in a circular cylinder, *Computers & Mathematics with Applications*, 56 (2008) 3096-3108.
[28] Qi, H., Xu, M., Stokes' first problem for a viscoelastic fluid with the generalized Oldroyd-B model, *Acta Mechanica Sinica*, 23 (2007) 463-469.
[29] Jiang, Y., Qi, H., Xu, H., Jiang, X., Transient electroosmotic slip flow of fractional Oldroyd-B fluids, *Microfluidics and Nanofluidics*, 21 (2017) 7.
[30] Wang, S., Zhao, M., Analytical solution of the transient electro-osmotic flow of a generalized fractional Maxwell fluid in a straight pipe with a circular cross-section. *European Journal of Mechanics - B/Fluids*, 54 (2015), 82–86.
[31] Guo, X., Qi, H., Analytical Solution of Electro-Osmotic Peristalsis of Fractional Jeffreys Fluid in a Micro-Channel, *Micromachines (Basel)*, 8(12) (2017), 341.
[32] Wang, X., Qi, H., Yu, B., Xiong, Z., Xu, H., Analytical and numerical study of electroosmotic slip flows of fractional second grade fluids. *Communications in Nonlinear Science and Numerical Simulation*, 50 (2017) 77-87.
[33] Awan, A.U., Hisham, M.D., Raz, N., The effect of slip on electroosmotic flow of a second grade fluid between two plates with Caputo-Fabrizio time fractional derivatives. *Canadian Journal of Physics*, 50 (2018) doi: 10.1139/cjp-2018-0406.